Talanta 134 (2015) 354–359

Contents lists available at ScienceDirect

Talanta

journal homepage: www.elsevier.com/locate/talanta

Determination of guanine and adenine by high-performance liquid chromatography with a self-fabricated wall-jet/thin-layer electrochemical detector at a glassy carbon electrode

Yaping Zhou [a,b], Hongling Yan [a], Qingji Xie [a,*], Shouzhuo Yao [a]

[a] Key Laboratory of Chemical Biology & Traditional Chinese Medicine Research (Ministry of Education of China), College of Chemistry and Chemical Engineering, Hunan Normal University, Changsha 410081, China
[b] College of Pharmacy, Zunyi Medical University, Zunyi 563000, China

ARTICLE INFO

Article history:
Received 30 August 2014
Received in revised form
19 November 2014
Accepted 20 November 2014
Available online 29 November 2014

Keywords:
High-performance liquid chromatography
Wall-jet/thin-layer amperometric electrochemical detector
Guanine
Adenine
Electrode-adsorption effect

ABSTRACT

A sensitive wall-jet/thin-layer amperometric electrochemical detector (ECD) coupled to high-performance liquid chromatography (HPLC) was developed for simultaneous determination of guanine (G) and adenine (A). The analytes were detected at a glassy carbon electrode (GCE) and the HPLC – ECD calibration curves showed good linearity ($R^2 > 0.997$) under optimized conditions. Limits of detection for G and A are 0.6 nM and 1.4 nM ($S/N=3$), respectively, which are lower than those obtained with an UV–vis detector and a commercial electrochemical detector. We have successfully applied this HPLC – ECD to assess the contents of G and A in hydrochloric acid-digested calf thymus double-stranded DNA. In addition, we compared in detail the analysis of G and A by cyclic voltammetry (CV) and by the HPLC – ECD system on both bare GCE and electroreduced graphene oxide (ERGO) modified GCE. We found that the adsorption of G and A on the electrode surfaces can vary their anodic CV peaks and the competitive adsorption of G and A on the limited sites of the electrode surfaces can cause crosstalk effects on their anodic CV peak signals, but the HPLC – ECD system is insensitive to such electrode-adsorption and can give more reliable analytical results.

1. Introduction

Nucleic acid is a kind of biomacromolecules of organism, which store and transmit genetic information in protein biosynthesis. Thus, it takes a critical part in great life phenomena such as growth, heredity, variation, and so on. Guanine (G) and adenine (A) are two important components found in nucleic acid and play crucial roles in physiological and pathological activies. Their levels are considered as important parameters for diagnosis of tumor, AIDS, epilepsy, myocardial cellular energy status, disease progress, and therapy responses [1–3]. Hence, the determination of G and A has great significance in clinical research and molecular biology investigation [4,5].

Until now, a large number of methods have been established for G and/or A analysis, including electrochemical methods [6–14], capillary electrophoresis [15], flow injection-chemiluminescence [16], micellar electrokinetic chromatography [17], resonance Rayleigh scattering [18], fluorimetric detection [19,20], and so on. High-performance liquid chromatography (HPLC) is one of the most widely used techniques for quantitative analysis in complicated matrices [21–27]. Due to its excellent selectivity and sensitivity, HPLC coupled with electrochemical detector (HPLC – ECD) may be a good choice for the quantitative analysis of electroactive compounds in complicated biological samples. As far as we know, the amperometric ECD, one of the main ECDs for HPLC (another commonly encountered ECD is the coulommetric ECD), can be classified into four categories, namely, thin–layer mode, wall–jet mode, open–tubular electrode mode, and in–tube electrode probe mode, according to the configuration of detection electrode against the eluent [28]. Among those modes, the thin–layer and wall–jet modes are the most common in the reported HPLC–ECD systems. However, inconvenience of the electrode rinse in the thin–layer mode and a limited response signal resulted from the transience of the HPLC liquid jetted onto the electrode surface in the wall–jet mode can restrict their effectiveness in electrochemical detection. Hence, a combination of wall–jet and thin–layer modes, namely, a wall–jet/thin–layer amperometric ECD, can well integrate the advantages of both modes and weaken their respective shortcomings, yielding an ECD with enhanced sensitivity and more convenient washing/refreshment of the working electrode

* Corresponding author. Tel./fax: +86 731 88865515.
E-mail address: xieqj@hunnu.edu.cn (Q. Xie).

http://dx.doi.org/10.1016/j.talanta.2014.11.042
0039-9140/

surface [28]. To the best of our knowledge, no investigation on such a self-fabricated wall–jet/thin–layer amperometric ECD for quantitative analysis of G and/or A has been reported to date.

Herein, we report a home-made integrated wall-jet/thin-layer amperometric ECD coupled to HPLC for the simultaneous determination of G and A at a glassy carbon electrode (GCE), as depicted in Scheme S1. Our detector here possesses the following advantages and significance. (1) The analytes are ejected from the HPLC outlet tube and reach the center of the working electrode, then flow around the electrode surface, thus we could improve the electrolysis efficiency and enhance the sensitivity by increasing the electrode area; (2) its simplicity and facile operation make the working electrode be treated easily and modified conveniently with any conductive and/or electrocatalytic material for wider applications. We will apply it to determine purine bases in hydrochloric acid-digested calf thymus double-stranded DNA (dsDNA) and compare its performance with an UV–vis detector and a commercial electrochemical detector. Furthermore, we will compare the influences of electrode adsorption of G and A in conventional cyclic voltammetry (CV) electroanalysis and HPLC – ECD analysis.

2. Materials and methods

2.1. Instruments and materials

The HPLC system comprised a LC-20AT binary high-pressure pump (Shimadzu, Kyoto, Japan), a UV–vis spectrophotometric detector SPD-20AV (Shimadzu, Kyoto, Japan) and a manual injector with a 20.0 μL sample loop. The commercial L-ECD-6 A electrochemical detector (Shimadzu, Kyoto, Japan) for HPLC, consisted of a glassy carbon plate working electrode, an Ag/AgCl reference electrode and a stainless steel nipple auxiliary electrode. The mobile phases were filtered and degassed by a SHB-3 type vacuum pump (Zhengzhou Dufu Instrument Factory, Zhengzhou, Henan, China) and the pH of buffer solution was measured with a Leici PHS-3C pH meter (Shanghai Precision & Scientific Instrument Co. Ltd., Shanghai, China). A self-fabricated wall-jet/thin-layer ECD and a CHI660A electrochemical workstation (Shanghai Chenhua Instrument Co. Ltd., Shanghai, China) was used for HPLC analysis, as schematically depicted in Scheme S1. We employed a three–electrode configuration consisting of a GCE as the working electrode (5 mm in diameter), a KCl-saturated calomel electrode (SCE) as the reference electrode and a carbon rod as the counter electrode. A plexiglass plate (0.25 cm in thickness) was pasted on the bottom of a plastic vessel and a hole of ca. 0.10 cm diameter was drilled in the plexiglass plate. The HPLC outlet tube was passed through the hole and its end was just horizontal to the upper surface of the plate. We pressed the working electrode firmly against the hole in plexiglass plate and the HPLC outlet tube was placed against the center of the working electrode. Thus the space between the working electrode surface and the plate can form a thin layer. All potentials are reported versus SCE unless otherwise specifically stated. Amperometric current-time curves were generated using a potentiostatic method with the accompanying software of the CHI660A electrochemical workstation.

G and A were obtained from Amresco (Solon, OH, USA). Calf thymus dsDNA and graphene oxide (GO) were purchased from Sigma (St. Louis, Missouri, USA) and Xianfeng Nanotechnology Inc. (Nanjing, Jiangsu, China), respectively. HPLC-grade methanol was purchased from Tianjin Damao Chemical Reagent Factory (Tianjin, China). Phosphate-buffered saline (PBS) solution was prepared with KH_2PO_4 and $K_2HPO_4 \cdot 3H_2O$ (Sinopharm Chemical Reagent Co. Ltd., Shanghai, China) unless otherwise specified, the pH of which was adjusted to the desired value by concentrated phosphoric acid (Sinopharm Chemical Reagent Co. Ltd., Shanghai, China). Other chemicals used were of analytical grade or better quality and Milli-Q ultrapure water ($>$ 18 MΩ cm, Millipore, Boston, Massachusetts, USA) was used throughout the experiments.

2.2. Chromatographic conditions

The HPLC analysis was carried out on a Shim-pack VP-ODS (i.d. 5 μm, 150 × 4.6 mm) column (Shimadzu, Kyoto, Japan) and the flow rate was 1.0 mL min^{-1}. An isocratic elution of the mobile phase consisting of 0.01 M PBS (pH 7.00)-methanol (85:15, v/v) was used. Prior to use, the mobile phase was filtered through a 0.22 μm membrane and degassed by a vacuum pump. All sample solutions should be filtered through 0.22 μm filters before injection. The column temperature was ambient and the electrochemical detector was placed behind the UV detector operating at 254 nm.

2.3. Preparation of electroreduced graphene oxide modified GCE

The accurately weighed amount of GO was dispersed in 0.10 M PBS (pH 7.40) consisting of $NaH_2PO_4 \cdot 2H_2O$ and $Na_2HPO_4 \cdot 12H_2O$ and subsequently ultrasonicated for 30 min to obtain 1 mg mL^{-1} GO dispersion. Prior to use, the GCE was first polished with 1.0 and 0.05 μm alumina slurry sequentially and then ultrasonically washed in ethanol and water for 5 min, respectively. The electroreduced graphene oxide modified GCE (ERGO/GCE) was prepared by immersing the cleaned GCE into GO dispersion and then scanning 10 cycles in a potential range from 0 to −1.50 V with a scan rate of 25 mV s^{-1}.

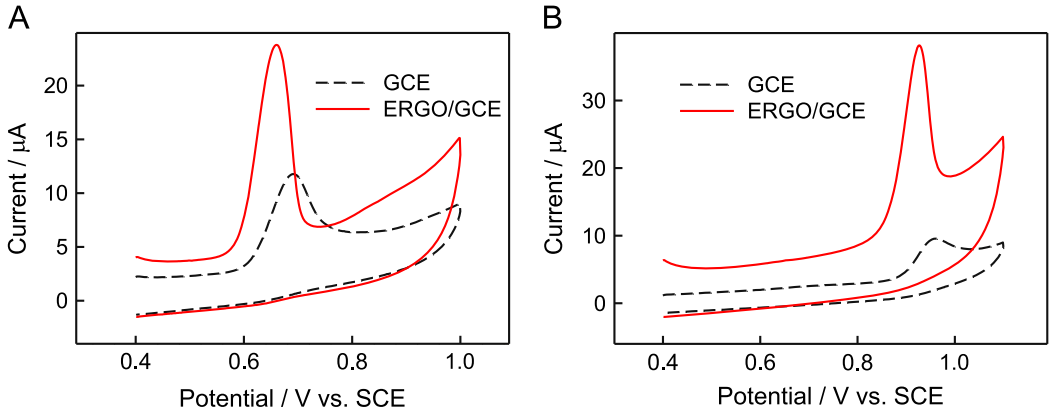

Fig. 1. Cyclic voltammograms of 50.0 μM G (panel A) and 50.0 μM A (panel B) in 0.10 M PBS (pH 7.00) obtained at the bare GCE (black dashed curves) and the ERGO/GCE (red solid curves). Scan rate: 100 mV s^{-1}.

2.4. Standard solution and sample preparation

Stock solutions (1.00×10^{-2} mol L^{-1}) of G and A were prepared by dissolving the accurately weighed amount of the substances in 0.10 M KOH aqueous solution. Further dilutions were made with mobile phase to prepare working standard solutions of G and A. Fresh solutions of all standards were prepared weekly and stored at 4 °C for future use.

Calf thymus dsDNA was hydrolyzed according to a previous report [29] for quantification of G and A. In brief, 3.0 mg of dsDNA was digested using 1.0 mL of 1.00 mol L^{-1} HCl in a sealed 10.0 mL glass tube. After heating in a boiling water bath for 80 min, the solution was adjusted to pH 7.00 with 1.0 mL of 1.00 mol L^{-1} NaOH. The solution was then filtered through a 0.22 μm membrane prior to the HPLC analysis.

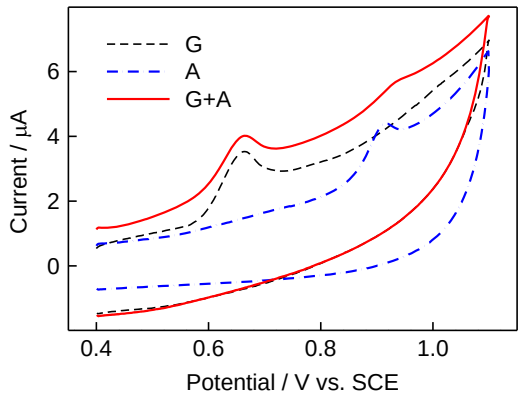

Fig. 2. Cyclic voltammograms of the bare GCE in 0.10 M PBS (pH 7.00) after being immersed in 50.0 μM G (black dashed curves), 50.0 μM A (blue dashed dotted curves) and the mixture solution containing 50.0 μM G and 50.0 μM A (red solid curves) for 10 min, respectively. Scan rate: 100 mV s^{-1}.

3. Results and discussion

3.1. Optimization of the HPLC separation conditions

For optimizing separation of G and A, the predicted composition of the mobile phase would consist of methanol and buffer solution on the basis of a previous article [30]. To ensure a sufficient ionic conductivity of the mobile phase for electrochemical detection, the aqueous part of mobile phase contained 0.01 mol L^{-1} PBS. First of all, we evaluated the influence of the methanol percentage in the mobile phase containing PBS of pH 7.00 on the retention characteristics of the analytes. With the increase of methanol content, the overall time of analysis was saved, but the separation efficiency was decreased and a complete separation of G from A could not be achieved with the mobile phase consisting of up to 40% methanol, as shown in Fig. S1. To obtain a good separation result in a short time, we select the mobile phase consisting of 15% methanol, which gave minimum symmetry factors of peaks and good peak shapes, as optimum for further studies.

The effect of the pH of PBS compatible with the column pH range of stability (from 3.00 to 7.00) was also tested. Well-separated peaks were obtained at pH from 4.00 to 7.00. In

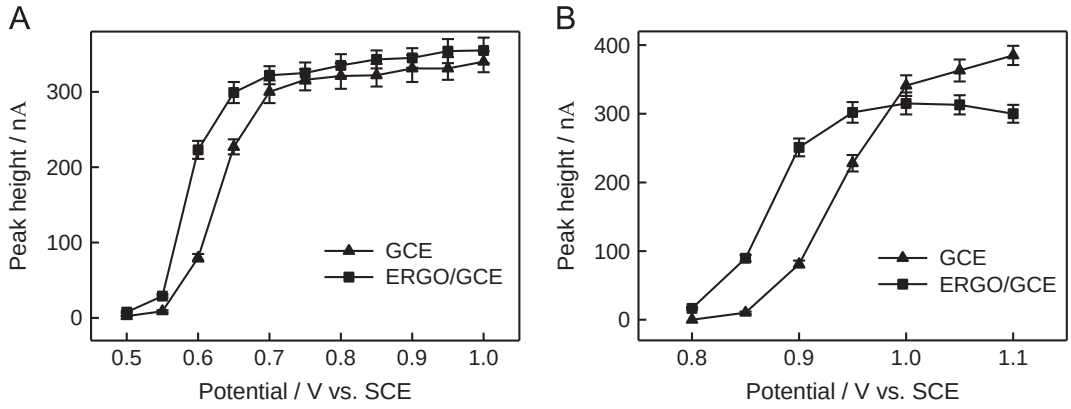

Fig. 3. Peak heights of 50.0 μM G (panel A) and 50.0 μM A (panel B) detected at the bare GCE and the ERGO/GCE in our HPLC-ECD. The diameter of GCE is 3 mm. Shim-pack VP-ODS (5 μm, 150 × 4.6 mm) column, 0.01 mol L^{-1} PBS (pH 7.00) containing 15% methanol (v/v) as mobile phase, 1.0 mL min^{-1} flow rate, injected volume: 20.0 μL.

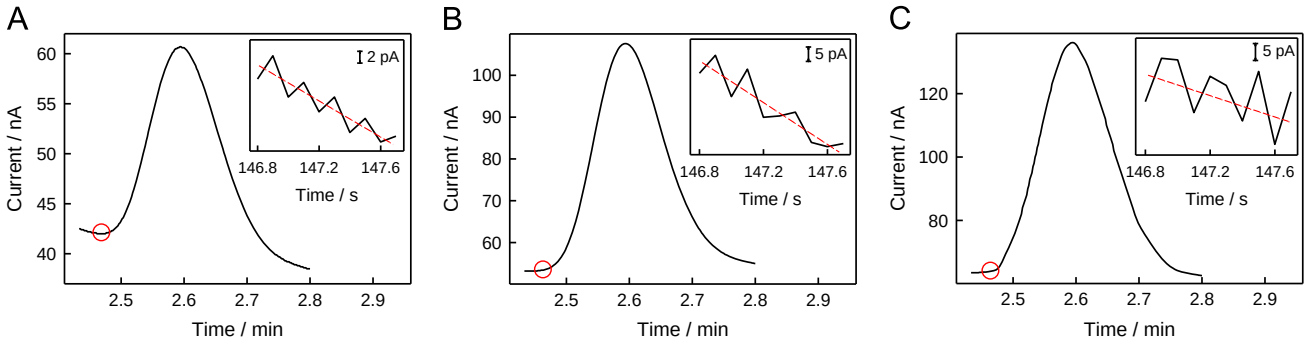

Fig. 4. Chromatograms of 1.00 μM G obtained by HPLC-ECD at a GCE of 3 (A), 5 (B) or 7 (C) mm diameter. Inset with the red dashed central line shown is the magnification of the red circled part. Chromatographic conditions are same as those in Fig. 3, applied potential: 1.00 V.

addition, we found that the efficiency of the chromatographic system expressed in terms of the number of theoretical plates increased with increasing pH of the PBS. Therefore, the mobile phase consisting of PBS (pH 7.00) and 15% (v/v) of methanol, which represents a good compromise between a well separation and a reasonable analysis time, is chosen for separating G and A.

3.2. Electrochemical detection

It is well-known that modifying the electrode surface with conductive and/or electrocatalytic materials is a highly effective method for increasing electroanalytical signals and enhancing detection sensitivity, which has been often utilized in electrochemical analysis. Thus, we first analyzed G and A by cyclic voltammetry (CV) on both bare GCE and ERGO/GCE. From the cyclic voltammograms of G and A shown in Fig. 1, we observed the greatly increased oxidation peak currents and negatively shifted oxidation peak potentials of both analytes on the ERGO/GCE, as compared with those on the bare GCE, demonstrating that the ERGO/GCE exhibits excellent electrocatalytic activity toward oxidation of both analytes. Furthermore, it is observed that there are excellent linear relationships between the anodic peak current and scan rate for both analytes ($R^2 > 0.995$) at the bare GCE and the ERGO/GCE, indicating that the oxidations of G and A on both bare GCE and ERGO/GCE are surface-controlled processes (Fig. S2) [31]. In other words, the adsorption of G and A on the electrode will largely influence their electrooxidation signals. Hence, the effect of competitive adsorption of G and A at the working electrode on their simultaneous analysis must be considered in conventional electroanalysis methods. Here, we found that, after the electrode being immersed in the mixture solution containing G and A for 10 min, the peak currents of both analytes obtained at the bare GCE in 0.10 M PBS (pH 7.00) greatly decreased (43.6% for G and 74.5% for A), as compared with those after the electrode being immersed in the single analyte solution with the same concentration, as shown in Fig. 2, which demonstrates that there was competitive adsorption between G and A on the limited sites of the bare GCE surface and it went against the accurate analysis for both analytes in their mixture solution. Based on the above results, we must emphasise that the presence of a highly competitive adsorbate(s) can notably influence the conventional electroanalysis (e.g. CV) results obtained from the surface-controlled faradaic process of the electroactive analyte, and thus one should pay great attention to consider and avoid such systematic errors in conventional electroanalytical methods. However, the HPLC coupled with ECD may be logically insensitive to such electrode-adsorption and give more accurate and reliable analytical results due to the following reasons: (1) the efficient separation of the analytes before their detection should intrinsically contribute to avoid the competitive adsorption; (2) there may not be enough time for one analyte or other adsorbates to occupy all the adsorption sites on the electrode in a flowing system, and the solution flowing may effectively make the adsorbates desorbed before detection of other analytes. Hence, we analyzed G and A with our HPLC – ECD system.

Fig. 3 shows the HPLC – ECD responses of G and A on the bare GCE and ERGO/GCE of varying potential under the optimized separation conditions described in the previous section. We can see that, the peak heights of G and A at the bare GCE dramatically increased at potential above 0.50 V and 0.80 V, respectively, then the peak heights reached the plateau at 0.70 V for G and 1.00 V for A. When the potential was higher than 1.00 V versus SCE, the peak height of A continued to raise, but a significant increase in background current occurred and some other substances maybe responded on the electrode. Therefore, 1.00 V is selected as the optimum potential for simultaneous determination of G and A in the HPLC – ECD system. Similarly, the peak heights of G and A at the ERGO/GCE also dramatically increased, and were much higher than those at the bare GCE as expected when the applied potential was increased from 0.50 V to 0.65 V and 0.80 V to 0.95 V, respectively. Then the peak heights at the ERGO/GCE achieved the plateau at 0.65 V for G and 0.95 V for A, both negative to the plateau potentials of both analytes at the bare GCE (0.70 V for G and 1.00 V for A), confirming the high electrocatalytic activity of ERGO toward both analytes oxidation. However, the peak heights of both analytes at the ERGO/GCE were almost the same as those at the bare GCE when the potentials were applied above the plateau potentials. This finding suggests that the ERGO as an electrocatalytic material does not produce obvious advantage when the applied potential is sufficiently positive to provide enough energy for promoting electron transfer reaction. This interesting finding also confirms that the adsorption sites on the bare GCE per unit geometric area were sufficient to accommodate adsorbed G or A molecules of such a small solution-concentration

Table 1
Signals, noises, and relevant parameters for HPLC–ECD detection of 1.00 μM G at disk GCEs of varying diameter under the optimum conditions.

Diameter (mm)	Current background (nA)	Data–recording scale of the instrument (A V^{-1})	Signal (nA)	Noise (pA)	S/N	LOD (nM)
3	42.3	1×10^{-8}	20.3	2.5	8120	2.4
5	53.5	1×10^{-8}	54.2	5.0	10840	0.6
7	63.2	1×10^{-7}	70.2	7.5	9360	1.5

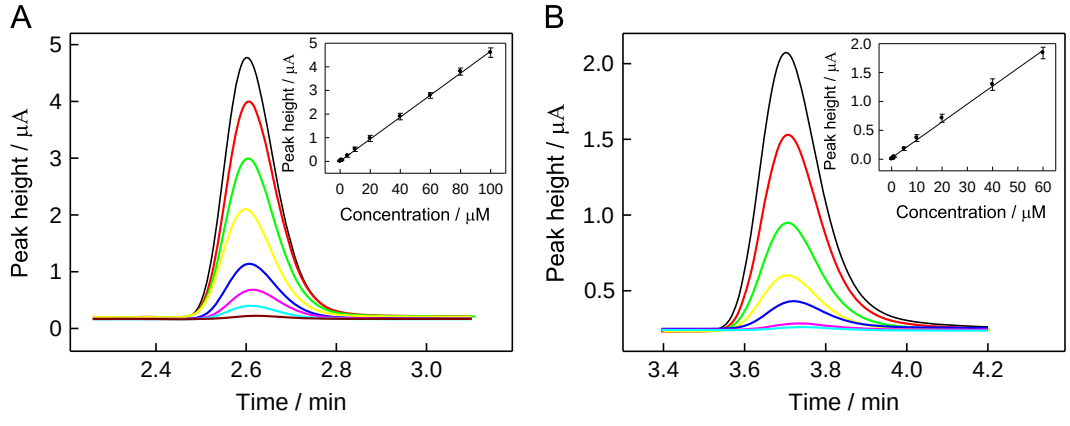

Fig. 5. Chromatograms and corresponding calibration curves (Insert) of G (panel A) and A (panel B) obtained with HPLC-ECD at the bare GCEs (5 mm in diameter). Chromatographic conditions are same as those in Fig. 4.

per unit time for their steady-state electrooxidation, which provided very limited adsorbates to access the unit geometric area of the electrode surface from the stationary or flowing solution, thus the effect of the ERGO-enlarged real surface area (geometric area not increased) was minor. In contrast, the electrocatalysis effect of ERGO was notable in the CV experiments shown in Fig. 1, because CV is not a steady-state but a transient electrochemical method and the electrode kinetics take effect. For convenience, the bare GCE is thus utilized for simultaneous determination of both analytes at 1.00 V (steady-state experiment) in the following HPLC–ECD experiments.

Obviously, the amperometric signal for both anayltes can be enhanced by increasing the geometric area of the detection electrode, since an electrode with a larger geometric area can capture more analyte molecules for electroanalysis. However, an enlarged geometric area of the detection electrode must result in a higher current background (capacitive currents and electrolytic currents of electroactive impurities), which prevents the selection of a small data-recording scale of the instrument to precisely record a small response signal, and thus the apparent noise level has to be high, as discussed in our previous work [28]. Therefore, examination of the electrode area regarding the signal and noise level is very important for optimizing the analytical performance of our ECD during detection of G and A. We investigated the HPLC–ECD responses of G at GCEs with varying geometric areas (Fig. 4) and the detailed data is summarized in Table 1. As expected, the HPLC–ECD peak height of G increased with the augment of geometric area of the detection electrode. However, a larger sum of response-signal plus signal-background at larger-geometric-area electrodes required a larger data-recording scale and resulted in a larger apparent noise (less precision of data), which could unfavorably decrease the signal-to-noise ratio (S/N) and increase the limit of detection (LOD). From the data listed in Table 1, we found that the S/N of the 5 mm diameter GCE was the largest, so we selected the GCE of 5 mm diameter for simultaneous HPLC–ECD analysis of G and A.

The influence of the flow rate in the range from 0.6 to 1.2 mL min^{-1} was also studied, as shown in Fig. S3. A lower flow rate resulted in increases in the peak area and the retention time due to the time-lengthened contact of the analytes with the electrode. On the other hand, the peaks suffered from broadening. Hence, we kept the flow rate at 1.0 mL min^{-1}.

A representative ECD chromatogram of a standard mixture obtained under the optimum conditions is shown in Fig. S4, accompanied by the UV detection chromatogram (UV detection at first in the HPLC eluent). Our ECD can yield two well-defined HPLC peaks within 5 min.

Table 2
Parameters of linear regression analysis and LODs obtained by different HPLC detectors.

Analyte	Regression equation[a]	RSD of sensitivity (%, $n=3$)	Linear range (μM)	R^2	LOD (nM)
Self-fabricated ECD					
G	$y=46.5x+14.3$	1.3	0.01–100	0.9996	0.6
A	$y=31.0x+24.2$	1.6	0.05–60.0	0.9972	1.4
UV-detection					
G	$y=2.03\times10^3x-142$	2.1	0.10–100	0.9998	21
A	$y=1.70\times10^3x-285$	1.7	0.10–100	0.9998	35
Commercial ECD					
G	$y=3.23\times10^3x+455$	1.5	0.10–40.0	0.9988	18
A	$y=9.63\times10^2x+194$	1.9	0.10–10.0	0.9966	65

[a] y and x represent the peak height (nA in self-fabricated ECD and μV in UV-detection and commercial ECD) and the concentration of the analytes (μM), respectively.

Table 3
Intra-day and inter-day variability of G and A detection by our HPLC-ECD.

Analyte	Concentration (μM)	RSD (%)	
		Intra-day ($n=5$)	Inter-day ($n=3$)
G	0.50	1.7	2.8
	5.00	2.5	3.3
	50.0	2.7	3.7
A	0.50	2.1	3.2
	5.00	2.4	3.6
	50.0	2.9	3.9

3.3. Analytical performance and application

Calibration dependences for both analytes were measured under the optimum conditions and the calibration curves were constructed by plotting the peak heights against the concentrations of analytes, as shown in Fig. 5. For comparison, UV detection at 254 nm and commercial ECD were also carried out and the parameters of the regression equations are summarized in Table 2. The linear ranges for G and A obtained with the self-fabricated ECD were 0.01–100 μM and 0.05–60.0 μM, respectively. The linear regression coefficients for both analytes were greater than 0.997, which are comparable with those obtained by UV detection and commercial ECD (Table 2). The LOD is defined here as the analyte concentration at which a signal of three folds of the

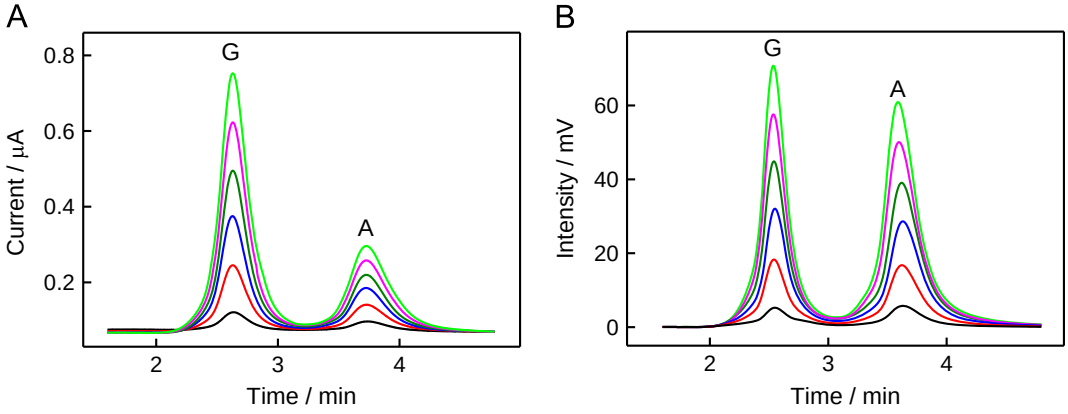

Fig. 6. Typical chromatograms of 100-fold diluted calf thymus dsDNA hydrolysates (black curves) and the diluted hydrolysates spiked with 20 (red curves), 40 (blue curves), 60 μM (dark green curves), 80 μM (pink curves) and 100 μM (green curves) G and A obtained by our HPLC-ECD (panel A) at the bare GCE (5 mm in diameter) and HPLC-UV detection (panel B) at 254 nm. Chromatographic conditions are same as those in Fig. 4.

Table 4
Determination results and recoveries for G and A in 100-fold diluted calf thymus dsDNA hydrolysates obtained with our HPLC-ECD and HPLC-UV detection[a].

Analyte	Found (μM)	RSD (%)	Added (μM)	Found (μM)	RSD (%)	Recovery (%)
Self-fabricated ECD						
G	7.46 ± 0.14	1.9	40.0	40.9 ± 0.54	1.3	102
			60.0	59.9 ± 0.68	1.1	99.8
			80.0	78.6 ± 1.47	1.9	98.3
			100	96.3 ± 1.39	1.4	96.3
A	10.6 ± 0.23	2.2	40.0	39.1 ± 0.47	1.2	97.8
			60.0	56.1 ± 0.73	1.3	93.5
			80.0	81.6 ± 1.24	1.5	102
			100	98.7 ± 2.26	2.3	98.7
UV-detection						
	8.02 ± 0.21	2.6	40.0	38.6 ± 0.62	1.6	96.5
			60.0	60.8 ± 0.82	1.3	101
			80.0	76.3 ± 1.54	2.0	95.4
			100	97.7 ± 2.34	2.4	97.7
	11.3 ± 0.28	2.5	40.0	38.1 ± 0.72	1.9	95.3
			60.0	58.4 ± 0.85	1.5	97.3
			80.0	82.9 ± 1.64	1.9	104
			100	98.2 ± 2.17	2.2	98.2

[a] Data expressed as mean value ± standard deviation (n=3).

background noise is obtained (S/N=3). As listed in Table 2, the LODs for G and A obtained with self-fabricated ECD are estimated to be 0.6 nM and 1.4 nM, respectively, which are lower than most of the reported values from some other typical methods (Table S1). In addition, the good separation of the two electroactive analytes by HPLC and the intrinsic insensitivity to the interferences brought by competing electrode-adsorption should make our method highly selective.

The reproducibility of the method was examined by performing repeated injections of the analyte standards on one day or on three consecutive days, and the results are listed in Table 3. G and A at three different concentrations were determined with both intra-day (n=5) and inter-day (n=3) relative standard deviations (RSDs) less than 4%, suggesting the good precision of the proposed method.

To validate the applicability of the self-fabricated ECD in HPLC−ECD, hydrochloric acid-digested calf thymus dsDNA was analyzed. We measured the contents and evaluated the recoveries of G and A in 100-fold diluted calf thymus dsDNA hydrolysates with standard addition method. For comparison, UV detection at 254 nm was also carried out. The chromatograms are shown in Fig. 6 and the results are summarized in Table 4. The recoveries of both analytes obtained with self-fabricated ECD ranged between 93.5% and 102%. In Table 4, the contents of G and A in calf thymus dsDNA were calculated as 20.7% and 29.3% (in the molar ratio, mol %), respectively. The value (G+C)/(A+T) of 0.71 was obtained for DNA sample, which agreed well with the values obtained using other electrochemical methods and coincided to the standard value of 0.77 [32], demonstrating good accuracy and reliability of our method.

4. Conclusions

In this article, we have developed a wall−jet/thin−layer ECD coupled to HPLC for the simultaneous detection of G and A at a GCE, and successfully assessed the contents of the analytes in calf thymus dsDNA with satisfactory results. In comparison with the commercial detectors, ease of electrode treatment and the better analytical performance of our ECD system make it promising in the fields of HPLC and flow-injection analysis for application in clinical diagnosis and the research of genetic information. In addition, we have found that the G and A can adsorb on both electrodes (bare GCE and ERGO/GCE), and the competitive adsorption on the limited sites of the electrode surfaces can notably influence the conventional electroanalysis (e.g. CV) results obtained from the surface-controlled faradaic process of the electroactive analytes, but the HPLC−ECD system is insensitive to such electrode-adsorption and can give more accurate and reliable analytical results.

Acknowledgments

This work was supported by the National Natural Science Foundation of China (21175042, 21475041), Hunan Lotus Scholars Program, Foundations of Hunan Provincial Education and Science/Technology Department, and State Key Laboratories of Chemo/Biosensing and Chemometrics and of Electroanalytical Chemistry.

Appendix A. Supporting information

Supplementary data associated with this article can be found in the online version at http://dx.doi.org/10.1016/j.talanta.2014.11.042.

References

[1] A. Pietrzyk, S. Suriyanarayanan, W. Kutner, R. Chitta, M.E. Zandler, F. D'Souza, Bioelectron 25 (2010) 2522–2529.
[2] P. Cekan, S.T. Sigurdsson, J. Am. Chem. Soc. 131 (2009) 18054–18056.
[3] F.Q. Yang, J. Guan, S.P. Li, Talanta 73 (2007) 269–273.
[4] F. Jelen, A.B. Olejniczak, A. Kourilova, Z.J. Lesnikowski, E. Palecek, Anal. Chem. 81 (2009) 840–844.
[5] A. Abbaspour, A. Ghaffarinejad, Electrochim. Acta 55 (2010) 1090–1096.
[6] L. Feng, X. Zhang, P. Liu, H. Xiong, S. Wang, Anal. Biochem. 419 (2011) 71–75.
[7] P. Wang, H. Wu, Z. Dai, X. Zou, Biosens. Bioelectron. 26 (2011) 3339–3345.
[8] K. Huang, D. Niu, J. Sun, C. Han, Z. Wu, Y. Li, X. Xiong, Colloids Surf., B: Biointerfaces 82 (2011) 543–549.
[9] T. Liu, X. Zhu, L. Cui, P. Ju, X. Qu, S. Ai, J. Electroanal. Chem. 651 (2011) 216–221.
[10] A.H. Kamel, F.T.C. Moreira, C. Delerue-Matos, M.G.F. Sales, Biosens. Bioelectron. 24 (2008) 591–599.
[11] H. Yin, Y. Zhou, Q. Ma, S. Ai, P. Ju, L. Zhu, L. Lu, Process Biochem. 45 (2010) 1707–1712.
[12] R. Ghavami, A. Salimi, A. Navaee, Biosens. Bioelectron. 26 (2011) 3864–3869.
[13] I. Balan, I.G. David, V. David, A.-I. Stoica, C. Mihailciuc, I. Stamatin, A.A. Ciucu, J. Electroanal. Chem. 654 (2011) 8–12.
[14] K. Huang, L. Wang, H. Wang, T. Gan, Y. Wu, J. Li, Y. Liu, Talanta 114 (2013) 43–48.
[15] F.Q. Yang, L. Ge, J.W.H. Yong, S.N. Tan, S.P. Li, J. Pharm. Biomed. Anal. 50 (2009) 307–314.
[16] E. Liu, B. Xue, J. Pharm. Biomed. Anal. 41 (2006) 649–653.
[17] W. Wang, L. Zhou, S. Wang, Z. Luo, Z. Hu, Talanta 74 (2008) 1050–1055.
[18] Q. Xu, Z. Liu, X. Hu, L. Kong, S. Liu, Anal. Chim. Acta 707 (2011) 114–120.
[19] L.M. Devi, D.P.S. Negi, Nanotechnology 22 (2011) 245502–245506.
[20] Y. Cui, J. Yu, S. Feng, Talanta 130 (2014) 536–541.
[21] B. Todd, J. Zhao, G. Fleet, J. Microbiol. Meth. 22 (1995) 1–10.
[22] J. Shi, H.F. Liu, J.M. Wong, R.N. Huang, E. Jones, T.J. Carlson, J. Pharm. Biomed. Anal. 56 (2011) 778–784.
[23] Y. Wei, L. Yue, Q. Liu, J. Chen, J. Xie, J. Chromatogr. B. 879 (2011) 1707–1712.
[24] B.J. Petteys, E.L. Frank, Chim. Acta 412 (2011) 38–43.
[25] J. Wang, T. Lin, J. Lai, Z. Cai, M.S. Yang, J. Chromatogr. B. 877 (2009) 2019–2024.
[26] N. Kochanowski, F. Blanchard, R. Cacan, F. Chirat, E. Guedon, A. Marc, J.-L. Goergen, Anal. Biochem. 348 (2006) 243–251.
[27] W. Mailinger, A. Baumeister, M. Reuss, M. Rizzi, J. Biotechnol. 63 (1998) 155–157.
[28] Y. Zhou, H. Yan, Q. Xie, S. Huang, J. Liu, Z. Li, M. Ma, S. Yao, Analyst 138 (2013) 7246–7253.
[29] H. Wang, H. Ju, H. Chen, Anal. Chim. Acta 461 (2002) 243–250.
[30] P.G.d. Moral, M.J. Arin, J.A. Resines, M.T. Diez, J. Chromatogr. B. 826 (2005) 257–260.
[31] W. Sun, J. Liu, X. Ju, L. Zhang, X. Qi, N. Hui, Ionics 19 (2013) 657–663.
[32] N. Davidson, The Biochemistry of the Nucleic Acids, seventh ed., Cox & Nyman, Norfolk, 1972.